

**CHARACTERIZING THE OPTICAL EFFECTS OF THE FINEST FRACTIONS OF THE SOLAR SYSTEM: NANOPHASE ABSORBERS IN TRANSPARENT AND SCATTERING MATRICES.** C. Legett IV<sup>1</sup>, T. D. Glotch<sup>1</sup> and P. G. Lucey<sup>2</sup>, <sup>1</sup>Geosciences Department, Stony Brook University, 255 Earth and Space Sciences Building, Stony Brook, NY 11794-2100 (carey.legett@stonybrook.edu), <sup>2</sup> Planetary Geosciences/SOEST, University of Hawaii.

**Introduction:** Nanophase (< 1  $\mu\text{m}$ ) absorbers in transparent and scattering matrices are common on the surfaces of planetary bodies, yet their optical effects are relatively poorly characterized. Nanophase optical effects dominate the near-infrared spectral properties of Martian dust [1,2] and space weathered regolith on airless bodies like the Moon, Mercury, and the Trojan asteroids [3–5]. Since extremely small particles have large spectral effects relative to similar abundances of larger particles [3], the lack of a well-validated quantitative understanding of these effects poses a serious barrier to accurately interpreting remote sensing data sets from many solar system bodies. Here, we present the preliminary results of an ongoing project to characterize and model the spectral effects of strong absorbers (amorphous carbon and nanophase metallic iron) and weaker absorbers (mafic silicates) in transparent (halite) and scattering (silica aerogel) matrices.

#### Methods:

**Aerogel Mixture Preparation.** Silica aerogel samples are purchased as powders with a stated size of 200-700  $\mu\text{m}$ . The powders are baked overnight at 600  $^{\circ}\text{C}$  to remove surface methyl groups formed during production then cooled and a portion sieved in an ATM Sonic Sifter to yield a > 250  $\mu\text{m}$  size fraction. We then place an aliquot in a Retsch PM 100 agate planetary ball mill and alternately grind and sieve until sufficient quantities of 125-250  $\mu\text{m}$ , 90-125  $\mu\text{m}$ , 63-90  $\mu\text{m}$ , 32-63  $\mu\text{m}$ , and < 32  $\mu\text{m}$  fractions have been produced. BET surface area analysis is carried out on the bulk material after baking and on each size fraction after grinding and sieving in order to ensure that the aerogel structure hasn't been significantly altered through the grinding process. We then prepare mixtures of aerogel and amorphous carbon at 0.01, 0.1, and 0.5 wt% carbon at each size fraction and place them in a vacuum oven at 150  $^{\circ}\text{C}$  for 5-7 days to remove any adsorbed water.

**Halite Mixture Preparation.** Halite samples are prepared in much the same way as the aerogel samples, with the exclusion of the overnight bakeout at the beginning of the process. Additionally, we use a shatter-box-style agate puck mill to grind the halite to a < 32  $\mu\text{m}$  fraction that is then separated through Stokes settling in 2-propanol to retrieve the < 1  $\mu\text{m}$  size fraction. We then prepare mixtures with amorphous carbon

(~400 nm particle size) at 0.1, 0.5, 1, 2, and 5 wt%, and olivine, pyroxene, and flood basalt powders (individually, all < 1  $\mu\text{m}$  size fractions) at 1, 2, 5, 10, 25, 50, and 75 wt%.

**MIR Emissivity Measurements.** Mid-infrared (225-2250  $\text{cm}^{-1}$ ) emissivity measurements are carried out on a Nicolet 6700 FTIR using a CsI beamsplitter and a deuterated L-alanine doped triglycine sulfate (DLATGS) detector with a CsI window. Spectra are collected and calibrated using blackbody calibration targets in the manner of [6]. In order to achieve high signal to noise ratios, 1024 scans at the slowest available optical velocity are averaged for aerogel samples, and 256 scans are averaged for halite samples.

**VNIR Reflectivity Measurements.** Visible and near-infrared (350-2500 nm) reflectance measurements are acquired using the Vibrational Spectroscopy Laboratory's ASD Fieldspec3 Max spectrometer with incidence and emergence angles of 30 $^{\circ}$  and 0 $^{\circ}$  respectively. Sample spectra are referenced to a diffuse spectralon disk and splice corrected for small offsets at detector band edges. In order to achieve high signal to noise ratios, we average 900-1500 scans for each sample.

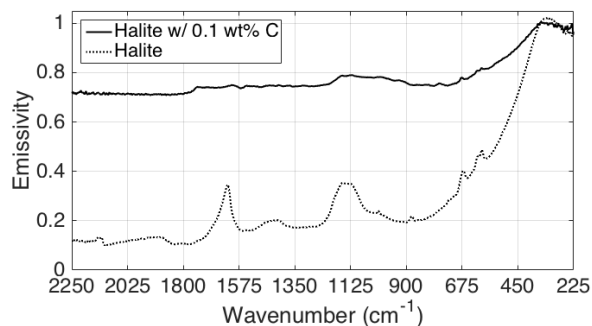


**Figure 1.** MIR emissivity of < 32  $\mu\text{m}$  size fraction of halite (bottom, dashed line) and halite with 0.1 wt% amorphous carbon added (top, solid line)

**Preliminary Results:** The features in the MIR emissivity of the < 32  $\mu\text{m}$  halite powder (Figure 1) match well with examples from the literature (e.g. [7]) and the addition of amorphous carbon has the expected effect of increasing emissivity and decreasing spectral contrast. It takes only 0.1 wt% carbon to raise the emissivity from a low near 0.1 to ~0.7. The two sharp peaks near 675 and 600  $\text{cm}^{-1}$  and the large peak near 1600  $\text{cm}^{-1}$  are likely due to adsorbed water and/or OH.

The corresponding VNIR reflectance spectra in Figure 2 show similar results, with the addition of carbon decreasing reflectance and significantly decreasing spectral contrast. The features above 1850 nm are unexpected for halite, and represent a contaminating phase in the sample. We plan to perform powder x-ray diffraction analysis in order to identify this phase and to determine a method by which it can be removed from our stock.

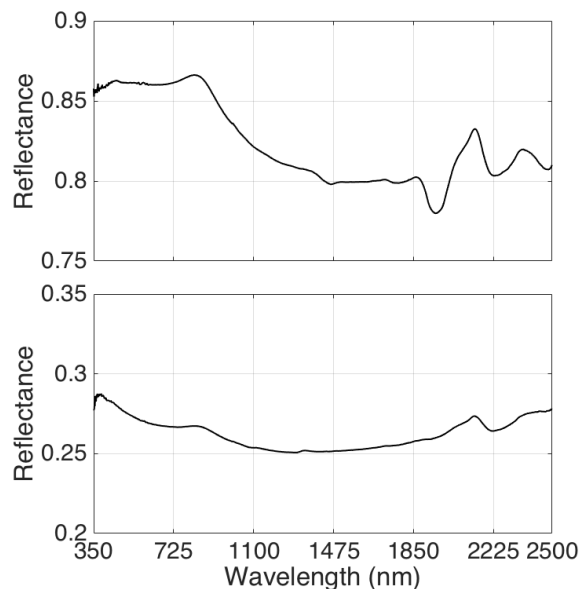


**Figure 2.** VNIR reflectance of  $< 32 \mu\text{m}$  halite (top) and  $< 32 \mu\text{m}$  halite with 0.1 wt% C (bottom). Note different y-axis ranges.

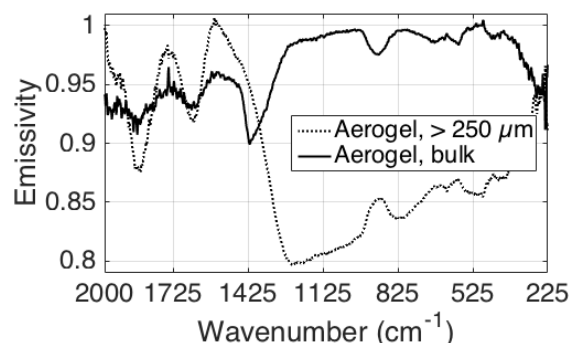


**Figure 3.** MIR emissivity of the bulk silica aerogel powder (dotted line, below legend) and the  $> 250 \mu\text{m}$  size fraction of the aerogel (solid line, above the legend).

In the aerogel samples, the bulk (unsieved) aerogel shows a lower emissivity at long wavelengths than the  $> 250 \mu\text{m}$  fraction does after sieving (Figure 3). Additionally, the Reststrahlen bands near  $900$  and  $600 \text{ cm}^{-1}$  in the  $> 250 \mu\text{m}$  fraction invert once the finer size fraction is removed. This is likely due to a shift in

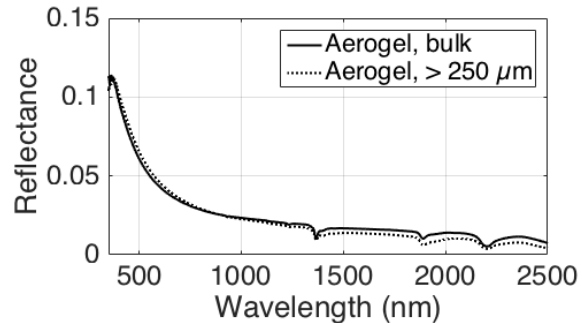


**Figure 4.** VNIR reflectance of the bulk silica aerogel powder (solid line) and the  $> 250 \mu\text{m}$  size fraction of the aerogel (dotted line).

scattering behavior from single scattering in the bulk sample to multiple scattering in the  $> 250 \mu\text{m}$  fraction. The VNIR reflectance spectra (Figure 4) are very dark due to light being scattered down into the transparent sample and away from the detector. The absorption features near  $1400$  and  $1900 \text{ nm}$  are characteristic of adsorbed water, while the feature at  $\sim 2200 \text{ nm}$  is due to silica. The bulk powder shows slightly lower reflectance at short wavelengths, and slightly higher reflectance and long wavelengths with the crossover occurring at  $889 \text{ nm}$ . Both samples show an increase in reflectivity at short wavelengths consistent with Rayleigh scattering [8].

**Conclusions and Future Work:** The preliminary data presented here demonstrate a few of the effects we are working to quantify in our larger set of experiments. The full set of mixtures and associated modeling work will allow us to better interpret the spectra of space weathered surface on airless bodies and chloride salt-bearing deposits on Mars and asteroids among many others. Additionally, we are developing an anaerobic procedure that will allow us to take reflectance and emissivity measurements of mixtures containing metallic iron nanoparticles without them oxidizing. Three component mixtures of halite with olivine, pyroxene, or basalt powders, and carbon or metallic iron are in progress along with the two component mixtures presented here.

**References:** [1] Bandfield, J.L. *et al. Science* (2003), **301**, 1084. [2] Morris, R.V. *et al. J. Geophys. Res.* (1989), **94**, 2760. [3] Hapke, B. (2012). [4] Hapke, B. *J. Geophys. Res.* (2001), **106**, 10039. [5] Pieters, C.M. *et al. Meteorit. Planet. Sci.* (2000), **35**, 1101. [6] Ruff, S.W. *et al. J. Geophys. Res.* (1997), **102**, 14899. [7] Lane, M.D. & Christensen, P.R. *Icarus* (1998), **135**, 528. [8] Clark, R.N. *et al. LPSC XLI* (2010).